Review of Discrete Element Modelling in Optimisation of Energy Consumption of a Single-Toggle Jaw Crusher

Peter Ndung'u Mwangi, Onesmus Mutuku Muvengei and Thomas Ochuku Mbuya

Abstract—This review paper has focused on optimisation of energy consumption during comminution process within the crushing chambers of a single toggle jaw crusher. Comminution has always been associated with operational efficiencies of below 10% due to energy dissipation during size-reduction through noise, heat and vibrations. Optimisation techniques such as altering the feed material characteristics through heat treatment have been proposed. However, such techniques increase the overall cost of aggregate production. Therefore, the most appropriate technique is optimising the jaw crusher dimensions such as the reduction ratio, throw and toggle speed using Genetic Algorithms (GA) and Discrete Element Modelling (DEM). The Rose and English model has been proposed for optimisation and is used together with GA. Even though the GA will reveal the optimal design parameters, it does not account for stresses, deflections and physical properties of the material and jaw crusher. This gives a strong incentive to use Discrete Element Method (DEM) in performance optimisation of the jaw crusher. DEM modelling has the capability of predicting the machine's power draw and process parameters. DEM models that have been proposed included Bonded Particle Model (BPM), Particle Replacement Model (PRM) and Fast Breakage Model (FBM). Of the three, BPM was found to be superior in compression induced fractures. PRM is suitable for impact crushing while FBM is ideal for flow-induced breakage.

Keywords—Bonded Particle Modelling, BPM, Comminution, Discrete Element Modelling, DEM, Efficiency, Jaw crusher optimisation, power consumption, size reduction,

I. INTRODUCTION

IN quarries, jaw crushers are at the first stage of comminution processing for the manufacture of aggregates. There are numerous types of crushers which have been developed over the years for various materials and required products. Experimental approaches have always been used to optimise and customize crushers. However, optimisation using experimental techniques, such as monitoring of mass flow, where particles break and how they break can be difficult. Basic input and output information such as feed size, feed rate, desired product size and power draw can be measured [1].

Comminution is the process of breaking rock particles into smaller fragments (aggregates). Aggregates are used as building materials in modern society. Naturally, the comminution process has been associated with low efficiency, which is typically less than 10%. This dissipative nature arises from random application of forces inside the machine and between the particles. Therefore, for the efficiency of the comminution process to be improved, the process has to be understood [2].

This gives a strong incentive to improve the production of high quality aggregates at low cost and minimal environmental footprint. To design and create more optimized jaw crushers, better evaluation tools need to be implemented in the design process. Experimental techniques require development of physical prototypes which are expensive and the test process is cumbersome. This has forced researchers to turn to virtual prototypes during design and evaluation [3].

Discrete Element Method (DEM) is one of the most robust computational technique that allows particle flows in crushing equipment to be simulated. The major advantage of DEM modelling is that it has the ability to simulate how particles flow through the equipment under controlled conditions and provide detailed predictions of specific outputs [4]. DEM provides a detailed fracture process during comminution. Simple geometries and single particles have been studied in the past by various authors. Usually, rock particles are formed by creating clusters of DEM particles which are bonded together.

Peter Ndung'u Mwangi, Department of Mechanical Engineering, JKUAT (phone: +254702688000; e-mail:peter.mwangi@jkuat.ac.ke, mwangipeter423@gmail.com).

Onesmus Mutuku Muvengei, Department of Mechanical Engineering, JKUAT (e-mail: mmuvengei@eng.jkuat.ac.ke).

Thomas Ochuku Mbuya, Department of Mechanical Engineering, University of Nairobi (e-mail: tmbuya@uonbi.ac.ke).

II. DISCRETE ELEMENT METHOD

A. Background

DEM simulation was first proposed by Cundall and Strack [5] as a numerical model capable of describing the mechanical behaviour of assemblies of discs and spheres. It is based on the use of an explicit numerical scheme where interaction of particles is monitored contact-by-contact and motion of the particles modelled particle-by-particle. An improvement was later made to DEM by introduction of Newton's second law of motion, linear hysteresis and use of contact models such as Hertz-Mindlin [3] [6].

DEM simulates discrete matter in a series of events known as time-steps. Once the particles are generated, the interaction between them is controlled using contact models and forces acting on all particles is calculated. Newton's second law of motion is then applied and the position of all particles can be calculated for next time-step [3]. DEM calculation loop is as shown in Fig 1.

B. Hertz-Mindlin Contact Model

In EDEM software, the no-slip Hertz-Mindlin contact model has two components; the normal force component and tangential force component. During simulation, the particles are

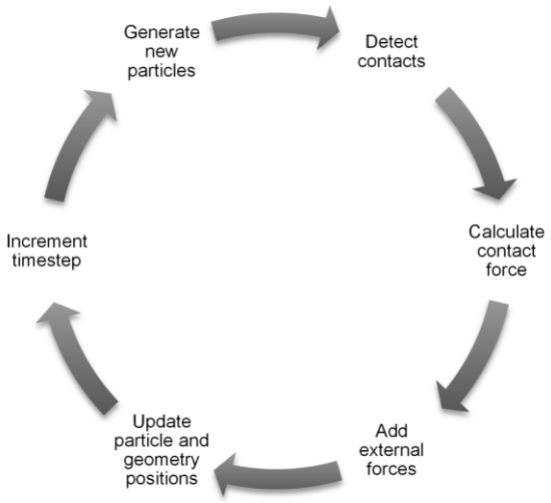

Fig. 1: Calculation loop used in DEM

allowed to overlap and the amount of overlap δx as well as the normal and tangential velocities at each contact point determine the collisional forces. A linear spring-dashpot model as shown in Fig 2 is used for the breakage algorithm. The

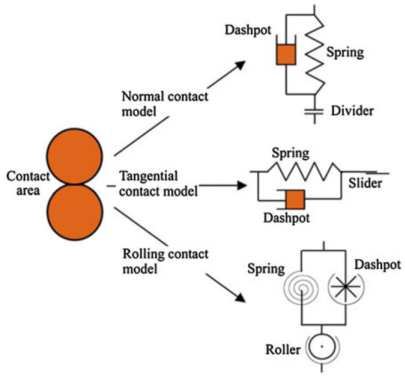

Fig. 2: Contact model between two spheres [7]

normal force is given by:

$$F_n = -k_n \Delta x + C_n v_n \mathbf{N} \tag{1}$$

Where,

$$C_n = 2\lambda\sqrt{m_{ij} k_n} \tag{2}$$

$$\lambda = \frac{-ln(\epsilon)}{\sqrt{\pi^2 + ln^2(\epsilon)}} \tag{3}$$

$$m_{ij} = \frac{m_i m_j}{m_i + m_j} \tag{4}$$

and

C_n= Damping coefficient of normal force in Ns/m.
k_n= Normal stiffness in N/m
ϵ= Coefficient of restitution.

Equation (1) has a linear spring to provide the repulsive force and a dashpot to dissipate a proportion of the relative motion. The term ϵ represents the coefficient of restitution which is defined as the ratio of the post-collisional to pre-collisional normal component of the relative velocity. In equation 4, the term m_{ij} represents the reduced mass of particles i and j with masses m_i and m_j respectively.
The tangetial force is given by:

$$F_t = min\left\{\mu F_n \sum k_t v_t \Delta t + C_t v_t\right\}\mathbf{N} \tag{5}$$

F_t and v_t are defined in the tangent plane at the contact point. The summation term in equation (5) represents an incremental spring that stores energy from the relative tangential motion and corresponds to the elastic tangential deformation of the contacting surfaces. The dashpot produces dissipation of energy in the tangential direction and represents plastic deformation of the contact in the tangential direction.

C. Calculation of stresses in DEM

DEM is only applicable for modelling the mechanical behaviour of discrete material such as rock and sand. In continuum mechanics, the stress-distribution cannot be obtained directly within the granular assembly. Homogenization or micro-macro averaging technique is used to calculate the stress tensor [7]. For an assembly of granular materials within a measurement volume (V), the stress tensor is defined as[8]:

$$\overline{\sigma_{ij}} = -\left(\frac{1-n}{\sum_{N_P} V^p}\right)\sum_{N_p}\sum_{N_p} |x_i^c - x_i^p| n^{(c,p)} F_j^c \tag{6}$$

In equation (6), the summation is taken over N_p particles whose centroids are located within the measurement volume V, n refers to the porosity of the measurement volume, V^p is the volume of a single particle; x_i^p is the location of the particle centroid; N_c is the number of contacts surrounding a single particle and $n^{(c,p)}$ is the unit normal directed from the particle center to the contact location x_i^c. The force acting at the contact as shown in Fig 3 is F_j^c.

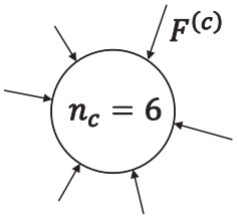

Fig. 3: Forces acting on a particle

1) Particle Stress Indexes: Grain crushing is induced by deviatoric stresses and the octahedral shear stress can be used to quantify a characteristic stress [9]. The stress index 1 based on the octahedral shear stress is as shown in equation (7).

$$\sigma_{i(1)} = \frac{1}{3}\left[(\sigma_1 - \sigma_3)^2 + (\sigma_1 - \sigma_2)^2 + (\sigma_2 - \sigma_3)^2\right]^{0.5} \tag{7}$$

Where, σ_1 is the major principal stress and σ_3 is the minor principal stress. In 2D, the intermediate stress is 0. Particles with just a few contact points can break because forces acting on them are not well distributed [10]. In addition, the crushing

of an individual particle is controlled by the largest contact force [11].

Stress index 2 is given by equation 8:

$$\sigma_{i(2)} = \sigma_t = \frac{2F_{max}}{\pi LD} \tag{8}$$

where F_{max} is the maximum normal contact force acting on the particle, D is the particle diameter and L is the thickness of the disk. Stress Index 3 can be defined as;

$$\sigma_{i(3)} = \frac{\sigma_1 - 3\sigma_3}{2} \tag{9}$$

where σ_o is the strength of the particle whose diameter D_o is known. The strength σ_o can be obtained by measuring the maximum contact force that can be carried by a single particle of a given diameter [12] [13].

2) Particle Strength: For a particle of diameter D, its strength can be defined as;

$$\sigma_{s(D)} = \sigma_o \left(\frac{D}{D_o}\right)^{\frac{-3}{m}} \tag{10}$$

D. Particle Breakage Models Used in DEM

Zheng and Tannant [14] modelled the grain breakage criteria of sand crushing using DEM. Laboratory tests were conducted so as to calibrate the discrete element model. The breakage grain criteria was observed using PFC2D software. Three methods of simulating grain breakage were proposed; Bonded Particle Model, Fast Breakage Model and Particle Replacement Model (or Population Balanced Model).

1) Bonded Particle Model (BPM): The bonded particle model (BPM) directly mimics the behaviour of cemented granular materials. A BPM particle is made up of coarse and fine particles which end up forming an irregular or regular shape [15]. The fine particles act as the cement (connections) which break when applied load goes beyond the pre-defined critical level [6]. BPM has been used to carry out investigations on the fracture behaviour of single rock particles. Potyondy demonstrated that this model had the ability of replicating the strain softening of granite in both confined and unconfined conditions [8].

The BPM model was first published by Potyondy and Cundall [8]. The particles bonded together are known as fraction particles while the resulting cluster is known as a meta-particle. A bi-modal particle size distribution is proposed by Johannes [3] as it forms realistic bonds. A high packing density should be achieved so as to eliminate the problem of mass-conservation due to the fact that the clustered rock particle might not be able to attain full solid density. During fragmentation, the bulk density of the meta-particle will change as new particles are formed. Unlike Particle Replacement Model, BPM is dependent on particle flow dynamics with the crushing chamber. Fig 4 depicts the forces and moments that act on a single BPM bond. These forces are given by:

$$\begin{aligned} \Delta F_b^n &= -k_b^n A_b v^n \Delta t \\ \Delta F_b^s &= -k_b^s A_b v^t \Delta t \\ \Delta M_b^n &= -k_b^s J \omega^n \Delta t \\ \Delta M_b^s &= -k_b^n J \omega^t \Delta t \end{aligned} \tag{11}$$

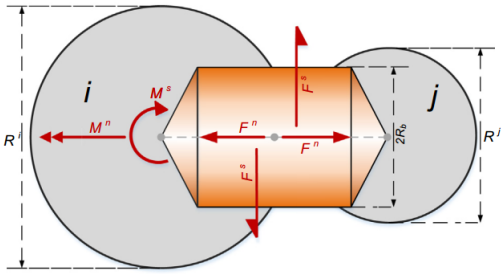

Fig. 4: Illustration of BPM forces and moments

where,

$$\begin{aligned} A_b &= \pi R_b^2 \\ J &= \frac{1}{2}\pi R_b^4 \\ I &= \frac{1}{4}\pi R_b^4 \end{aligned} \tag{12}$$

The terms k_b^s, k_b^n are shear and normal bond stiffness respectively, $v^n, v^t, \omega^n, \omega^t$ are normal and tangential velocities, and the normal and tangential angular velocities respectively. I, J and A_b are moment of inertia, polar moment of inertia and the cross-sectional area of the bond respectively. R_b is the bond radius and is a dependent of the smallest sphere in contact. Moment M_b and force F_b act in the normal direction (M_b^n and F_b^n) and shear direction(F_b^s and M_b^s) as shown in 11.

For fracture to occur, the applied normal and shear stresses must be greater than the critical stresses, σ_c and τ_c which are user-defined. The most crucial part of BPM is sphere size selection which make up the meta-particle. They could be normal distributions [16], bimodal distributions [3] or mono-dispersed [17].

Quist [3] used the BPM in modelling the crushing process within the cone-crusher. The simulation findings were compared against experimental findings. It was asserted that the particle flow behaviour through the crushing chamber looked realistic in comparison to what was observed from experiments. The simulations also revealed that the BPM approach captures the breakage process and the particles were able to react to different compressive breakage modes. The results obtained revealed that BPM simulation can be used to predict the mass flow and pressure but more work has to be performed on the post-processing for accurate power draw and size distribution predictions. The Single Particle Breakage (SPB) test was used as it gave more insight on how compression mode influences rock fracture. Legendre [2] used the SPB test and BPM model to assess the energy efficiency of a jaw crusher. The simulation was found to follow the operation of the real machinery during particle breakage. Potyondy [8] adopted the BPM in modelling of granite rock. It was concluded that BPM allows the cracks to form, interact with each other and coalesce into macroscopic fractures. The model was found to reproduce many features of rock behaviour such as elasticity, fracturing and strength increase with confinement. Jimenez [6] observed that BPM is capable of reproducing several aspects of particle breakage such as the force-deformation profile and how the particles

interact with the crushing walls. Diego [18] used BPM to simulate the mechanical behaviour of jointed rock masses. BPM was used to represent the intact rock material. It was concluded that this technique is suitable for simulating rock properties (fracture toughness, fracture strength, dilation angle, peak strength, etc.) which influence the comminution process.

2) Fast-Breakage Model: This technique has been used by Potapov and Campbell [19], Paluszny et al. [20] and in simulation of comminution equipment [21]. This method uses polyhedral elements to form DEM particles. It is a type of particle-replacement model. FBM is an instantaneous breakage model that uses the Laguerre-Voronoi tessellation to segment 3D polyhedral when the total energy after first collision is greater than the fracture energy. Bonds between individual particles are described using the linear hysteresis contact model as shown by Wu et al. [22]. The probability of breakage *P(E)* is described by the expression originally proposed by Vogel and Peukert [23]:

$$P(E) = 1 - exp[-S\left(\frac{d_i}{d_{i,ref}}\right)E_{cum}] \tag{13}$$

and,

$$\begin{aligned} E_{cum} &= E'_{cum} + E - E_{min} \\ E_{min} &= e_{min,ref}\left(\frac{d_{i,ref}}{d_i}\right) \end{aligned} \tag{14}$$

where, E'_{cum} is the accumulated energy in the particle just before the stressing event and E is the total specific energy of the collision during an impact event. S, $d_{i,ref}$ and $e_{min,ref}$ are model parameters which describe the amenability of the material to breakage, the reference size and the minimum energy for breakage respectively. The particle size is represented by d_i.

Jimenez [6] concluded that FBM describes the interaction between a particle and particle bed during impact crushing. In addition, this technique was found to have the ability to conserve mass and generate irregularly shaped fragments, hence making it suitable for simulations of large-scale comminution systems. However, FBM had limitations in describing the measured force-deformation profile from SPB as well as the progeny size distribution. Potapov [19] used FBM to study rock fracture and asserted that this method can be used to predict the size distribution for fragments larger than three element sizes. In addition, FBM is suitable for simulations involving flow-induced breakage of granular systems. Brosh et al. [24] applied FBM in CFD-DEM simulation of a size-distribution system. It was concluded that FBM is suitable for predicting size-reduction in systems where size-reduction is significant. However, FBM was found to require long computational time for simulations with large number of particles.

3) Particle Replacement Model: Particle Replacement Model (PRM), also known as Population Balanced Model (PBM), was first proposed by Cleary [25]. This model is based on the principle of replacing parent particles with progeny particles once they are subjected to a load greater than the critical strength [3] [6]. The set of progeny particles are of a predetermined size and shape. This model is analysed by Barrios et al. [26] using DEM software. Generation of progeny particles stops when the breakage process contains particles smaller than the minimum size. PRM does not take into account the particle flow dynamics as new particles are introduced at the same position as the broken parent particle i.e. particle dynamics are decoupled from the parent particle. Huiqi Li [27] explored the comminution process within the cone crusher using PRM. The results obtained from the simulations were compared against experimental findings. The effect of varying the Closed Side Set (CSS) and eccentric speed was investigated. Simulation results concurred with experimental data. However, the effect of fracture strength on energy consumption was not investigated. Jimenez [6] affirmed that PRM provided an ideal visualisation of size distribution of progeny particles from both SPB and particle bed experiments. However, it was not able to describe the measured force-deformation profile and there was no stochastic description of breakage probability. PRM gave poor descriptions of how the rock model interacted with the particle bed.

4) Weaknesses and Strengths of DEM Particle Breakage Models: BPM model has been used to simulate comminution process and model rocks by various authors [2] [3] [6] [8] [18] [28] [29]. BPM has been observed to reproduce superior power draw and force-deformation predictions than PRM and FBM techniques. In addition, BPM has been able to vividly describe the interaction between modelled rocks and compression walls. The cracks generated by BPM are able to interact with each other hence producing a more realistic approach in size-reduction simulations in comparison to PRM. However, BPM has been found to be less suitable for systems where large particle populations are required as it demands high computational power[6]. On its own, BPM is not capable of giving firm conclusions regarding power draw and size distribution and hence post-processing and analysis has to be done using MATLAB [3].

FBM is suitable for simulating size-reductions that are flow-induced [19][24]. In addition, this technique describes the interaction between particles and machinery walls during impact crushing. FBM has the ability to generate irregularly shaped fragments and conserve mass during comminution. However, just like BPM, this technique requires massive computational power for simulations with large number of particles. The force-deformation profile was also not presented using FBM and progeny size distribution was found to be inferior to those generated using BPM [6].

PRM is another DEM technique that has been used in size-reduction simulations [6] [25], [26] [27]. PRM has is suitable for simulations where impact crushing is dominant and large number of particles are to be simulated. PRM does not provide a good description of breakage probability and force-deformation profile.

Cabiscol et al. [30] used the multi-sphere feature within EDEM software to model uniaxial-compressed cylindrical tablets. It was discovered that the shape and edges of DEM tablet models affected the packing fraction hence needed to be done at high precision. Sliding and rolling friction were identified as the most sensitive parameters through a pouring experiment. Calibration for discrete element simulation was carried out using the data obtained from tumbling drum and

pouring tests i.e. the coefficient of restitution and Young's modulus. However, DEM was found to have the following limitations:

1) It was not capable of extrapolating input parameters for another system.
2) Some of the input parameters lacked physical meaning.

Metta et al. [31] used PBM to simulate a comill process. Experiments where the impeller speed was varied were conducted. It was observed that the impeller speed affected the particle size distribution and process parameters such as time required to attain a steady state and the hold up time. Therefore, an iterative algorithm that used mechanistic information from DEM and process variables from experiments was proposed. A breakage kernel was also created from the simulation.

III. POWER CONSUMPTION IN SINGLE TOGGLE JAW CRUSHERS

The single toggle jaw crusher is a comminution machine which has been associated with low energy efficiencies [2][32]. Legendre and Ron [2] demonstrated that the energy efficiency of a single toggle jaw crusher can be improved by either the pre-treatment of the feed material or altering the design parameters. Pre-treatment of feed material, however, was disregarded as it might increase the overall cost of comminution. Therefore, finding the optimal design machine parameters would be more realistic. Use of Evolutionary Algorithms and DEM was recommended as this method accounts for particle dynamics within the crushing chamber and will attempt to mimic an on-site jaw crusher [2]. Fig 5 shows the critical jaw crusher parameters that affect power consumption. Even

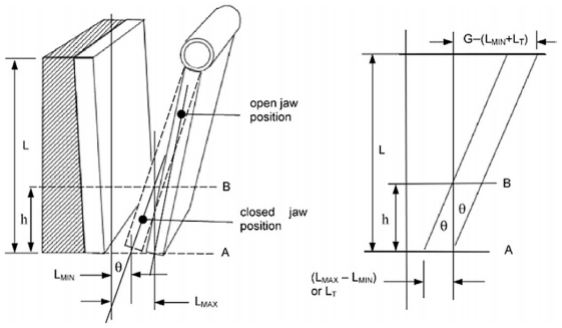

Fig. 5: Machine Parameters of a Single-toggle jaw crusher [2]

though jaw crusher design parameters such as the gape, throw, reduction ratio and operating speed affect power consumption, most authors have demonstrated that other factors such as weight of the swing jaw [32] [33] [34] and shape of the particle play an important role in power consumption [1] [35].

Bharule [33], Ramkrushna [34] and Sundar [36] investigated the effect of adding stiffeners to the swing jaw. Stiffeners increase the strength to weight ratio of the swing jaw. It was concluded that increasing the number of stiffeners will reduce the power consumption. Bharule [33], using CatiaV5R15, showed that stiffeners reduced energy consumption during comminution by 25%. Miller [37] designed a new crushing technique in which both crushing plates moved during crushing. This prototype reduced the fracture energy of the feed material but increased the cost of production i.e. the additional moving jaw required additional of extra components such as springs, bolts and machining/casting. The author reported that reduction ratio, material properties and production flow rate played a major role in power consumption.

A. Laws of Comminution Energy

In design, operation and control of comminution processes, it is necessary to correctly evaluate the comminution energy of solid materials [38]. Evaluating the comminution energy will enable engineers and manufacturers design efficient jaw-crushers and also predict the power draw of the machine. It has been observed that as the particle size decreases, the surface area of the particles increases. Therefore, the surface area before and after size reduction would indicate the amount of energy consumed during comminution[39]. Therefore,

$$dE = k[S^n dS] \tag{15}$$

where, E is the energy used during comminution, S is the surface area, k is a constant and a function of the crushing strength of the rock, and n is an exponent which has been determined by Rittinger, Kick and Bond [39].

Size reduction energy is expressed as a function of the feed size and product size. Four laws have been developed to model comminution energy; Rittinger's Law, Kick's Law, Bond's Law and Holmes' Law.

a) Rittinger's Law: Rittinger assumes that the energy consumed is directly proportional to the new surfaces created. Therefore, specific surface area is inversely proportional to the particle size. The specific comminution energy E/m is given by:

$$\frac{E}{m} = C_R(S_P - S_F) \ \textbf{[kJ/kg]} \tag{16}$$

Where, m is the particle mass, S_p and S_f are specific surface areas of product and feed respectively, and C_R is a constant that depends on the characteristics of the material.

b) Kick's Law: Kick law states that the energy required for comminution is related only to the ratio between feed size and product size.

$$\frac{E}{m} = C_K \ln\left(\frac{x_f}{x_p}\right) \ \textbf{[kJ/kg]} \tag{17}$$

Where x_p and x_f are the particle sizes of product and feed respectively while C_k is a constant. Equation (17) can be derived by assuming that the strength is independent on particle size and the energy for size reduction is proportional to the volume and size reduction is constant at each stage of comminution. This is in contradiction to Griffiths weakest link theory which mentions that as particles get smaller, they become more resistant to fracture [33].

c) Bond's Law: Bond approach has always been used in predicting the energy consumption during the size-reduction process. Bond Work Index coefficients cover almost the entire range of particles that are to be processed using comminution machinery[40]. Bond suggests that any comminution process

can be considered to be an intermediate stage in the breakdown of a particle of infinite size to an infinite number of particles of zero size. Bond's theory states that the total work useful in breakage is inversely proportional to the square root of the size of the product and feed particles:

$$W = W_i\left(\frac{10}{\sqrt{P_{80}}} - \frac{10}{\sqrt{F_{80}}}\right) \text{ [kWt/hr]} \quad (18)$$

Where, W is the work input, W_i is the Bond's work index, P_{80} is the Product size in microns at which 80% passes through the sieve[μm] and F_{80} is the Feed size in microns at which 80% passes through the sieve[μm]. From equation 15, the values of n depend on the type of application and are as follows:

- n= -2 (Rittinger)
- n= -1 (Kick)
- n= -1.5 (Bond)

Rittinger's expression n=-2 is applicable for coarse size reduction while for Kick n=-1 is suitable for finer size reductions. Bond's value of n=-1.5 covers almost the entire range of particles and has been accepted universerly [39].

However, the laws of comminution have a few weaknesses; they are not suitable for evaluation of primary crushing equipment processing large particle sizes, they only fit experimental data over a limited range of variables and suitable for only certain cases and Bond's work results in a conservative overdesign of the crushing plant. To counter these weaknesses, Single Particle Breakage analysis is currently being adopted to relate fracture energy and product size distribution to a materials property. There is enough evidence that a link exists between rock properties, energy consumption and performance of jaw crusher [32].

B. Single Particle Breakage

The mechanism of size reduction of solids is based on the fracture of a single particle and its accumulation during comminution operations[38]. The elastic strain energy, E $(Joules)$, input to a sphere up to the instant of fracture is given by:

$$E = 0.832\left(\frac{1-\nu^2}{Y}\right)^{\frac{2}{3}}(D)^{-\frac{1}{3}}(P)^{\frac{5}{3}} \quad (19)$$

The particle is subjected to compressive point loading. The tensile strength S (Pa) of the specimen is given by:

$$S = \frac{2.8P}{\pi D^2} \quad (20)$$

Substituting equation (20) to equation (19), the specific fracture energy E/m[**J/kg**] is given by:

$$\frac{E}{m} = 0.897\rho^{-1}(\pi)^{\frac{2}{3}}\left(\frac{1-\nu^2}{Y}\right)^{\frac{2}{3}}(S)^{\frac{5}{3}} \quad (21)$$

Where ρ is the density of the sphere in kg/m^3. When two spherical particles, 1 and 2, collide with each other, the maximum stress S_{max} generated inside the particles is expressed by a function of particle size, x, relative velocity ν (m/s) and mechanical properties:

$$S_{max} = 0.628\left(\frac{m_1 m_2}{m_1+m_2}\right)^{0.2}\mu^{0.4}\left(\frac{2}{D_1}+\frac{2}{D_2}\right)^{0.6}\left(\frac{1-\nu_1^2}{Y_1}+\frac{1-\nu_2^2}{Y_2}\right) \quad (22)$$

Where m_1 and m_2 are masses of particles 1 and 2 respectively in kg, μ is the relative velocity between the two particles in m/s, D_1 and D_2 are diameters of particle 1 and particle 2 respectively in m, ν_1 and ν_2 are poisson's ratio of particle 1 and 2, and Y is the Young's modulus ni MPa.

There is a direct relationship between fracture toughness and specific comminution energy [33]. From previous research [33] [37] [41], it is clear that a materials's reaction to applied load is dependent on size, shape and conditions under which the load is applied. Donovan [33] and Miller [37], demonstrated that bigger particles are easier to fracture than smaller ones. The shape of the feed material affects; the shear strength, realistic voidage(how the particles pack in the crushing chamber) inside the jaw crusher and, how and when the particles break [1][25].

C. Genetic Algorithms

Genetic algorithms (GAs) are numerical optimization algorithms which are inspired by both natural selection and natural genetics. A typical algorithm uses three operators, selection, crossover and mutation (chosen in part by analogy with the natural world) to direct the population (over a series of time steps or generations) towards convergence at the global optimum [42]. There are many types of Genetic Algorithms which come with different representations. The two most important GAs are the Simple Genetic Algorithm (SGA) and the Differential Evolution (DE) methods. It has been shown that a SGA code has a better potential of solving power consumption than a DE code [2]. Lee [43] used a genetic algorithm to optimize a jaw crusher performance theoretically. Theoretical efficiencies of 30%-40% were obtained. It should be noted that GA codes do note take into account the weight of the jaw plate, the friction between moving parts and vibrations induced during comminution. Therefore, GA codes should be used together with DEM for better optimisation.

The Rose and English [39] jaw crusher model should be adopted for flow rate and power consumption optimisation [2].

$$\dot{W} = 0.01195 W_i Q_A\left[\frac{\sqrt{G}-1.054\sqrt{L_{MIN}+L_T}}{\sqrt{G}\sqrt{L_{MIN}+L_T}}\right]\text{[kWh/t]} \quad (23)$$

Where, W_i is Bond's Work Index, Q_A is the actual flow rate in t/h, G, L_{MIN} and L_T are gape, closed side set and throw in m respectively. The maximum flow rate Q_A of a jaw crusher is calculated as:

$$Q_M = 60 L_t v_{cr} w(2L_{min}+L_t)\left(\frac{R}{R+1}\right)\rho f(P_k) f(\beta) S_c \text{ (t/h)} \quad \text{(A.1)}$$

The flow is affected by empirical functions $f(\beta)$ and $f(P_k)$. These functions are defined within a certain range; $0 \geq P_k \geq 1.2$ and $0 \geq \beta \geq 0.8$. The term S_c is a surface characteristic parameter related to the jaw crusher and has a range of $0.5 \leq S_c \leq 1$ [39].

The actual flow (Q_A) is the jaw crusher's real flow and is a function of operating velocity. It is given by:

$$Q_A = Q_M \frac{v}{v_{cr}} \text{ if } v \leq v_{cr} \text{ [t/h]} \quad (24)$$

and,

$$Q_A = Q_M \frac{v_{cr}}{v} \text{ if } v > v_{cr} \text{ [t/h]} \quad (25)$$

The critical velocity v_{cr} is calculated as[39];

$$v_{cr} = \sqrt{4414.5\left(\frac{G-(L_{min}+L_t)}{L}\right)\left(\frac{1}{L_t}\right)}\ [\textbf{rpm}] \quad (26)$$

The reduction ratio R is calculated as:

$$R = \frac{G}{Lmin} \quad (27)$$

D. Energy Efficiency Calculations

Legendre [2] approximated the energy consumed during comminution by measurement of surface area before and after size reduction of the feed.

$$\frac{dE}{dS} = kS^n \quad (28)$$

Where,

E= Indicator of the energy used in the comminution procedure.
S= The surface area before and after size reduction
K and n= Constants related to the crushing strength of the rock.

Tromans [44] defined the maximum ideal limiting efficiency based on compressive loading comminution machine, which generated a stress distribution inside a single particle as a result of a central crack flaw.

$$\eta_{limit} = \left[\frac{\sigma_x^2 - 2\nu(\sigma_x\sigma_y+\sigma_x\sigma_z)}{(\sigma_x^2+\sigma_y^2+\sigma_z^2)-2\nu(\sigma_x\sigma_y+\sigma_x\sigma_z+\sigma_y\sigma_z)}\right]\times 66\% \quad (29)$$

$$\sigma_x = \sigma_y = \frac{P}{\pi D^2}\left(\frac{6(1-2\nu)}{2+\sqrt{2}}\right) \quad (30)$$

$$\sigma_z = -\frac{P}{\pi D^2}\left(12-\frac{3}{\sqrt{2}}\right) \quad (31)$$

Where,

P= Loading Force, N
D= Particle Diametre, m
$\sigma_{x,y,z}$= Stresses along x,y and z axes
ν= Poissons ratio,-,typically ranging from 0 to 0.5

Tromans and Meech [44] showed that the increase in surface energy per unit of mass from particle fracture can be approximated by:

$$\Delta S_{En} = \frac{\gamma A_{Created}}{m} \approx \frac{6F_r\gamma}{\rho}\left(\frac{1}{D_{f_{Sm}}}-\frac{1}{D_{i_{Sm}}}\right)[\textbf{J/kg}] \quad (32)$$

Where,

γ = Fracture energy in J/m^2
$A_{Created}$ = New surface area created in m^2
$D_{i_{Sm}}$ and $D_{f_{Sm}}$= Initial and final surface mean diameter of particles in m respectively.
F_r = Dimensionless surface roughness factor that corrects for non-sphericity $[1 \leq F_r \leq 3]$

Assuming that the performance of the jaw crusher is ideal, there will be a continuous steady-state comminution process whose power consumption is given by:

$$\Delta S_{Power} = \Delta S_{En}(\textbf{kJ/kg}) \times 1(\textbf{kg/s})[\textbf{kW}] \quad (33)$$

Equation (33) assumes a normalised flow of 1 kg/s hence does not represent the actual power draw of a real comminution process. However, it is useful to monitor the influence of the machinery design parameters during comminution. Combining equation (32) and equation (33), the equipment total energy efficiency can be obtained by:

$$\eta_{EnergyTotal} = \frac{\frac{\Delta S_{En}}{E_{equipment}}}{\eta_{limit}} = \frac{\eta_{Classical}}{\eta_{limit}} \quad (34)$$

During comminution, the compressive strength, fracture toughness and tensile strength have the greatest influence on energy consumption. Korman observed that larger sized product particles were obtained when the uni-axial compressive strength of the material increased [45]. Kirankumar [46] explained the optimisation of a jaw crusher by modifying the frame, redesigning the crushing chamber and re-organizing the crushing parameters such as size reduction processes. However, high reduction ratios result in poorer shaped particles and higher production costs. Therefore, optimal reduction ratios should be used in jaw crusher designs.

IV. CONCLUSION

Discrete element modelling is a robust method in simulating the comminution process within the crushing chambers of comminution machines. From the literature, most researchers have used Bonded Particle Model and Population Balanced Model for simulation purposes. The BPM model is suitable for simulating size-reduction processes in machines such as the cone-crushers and jaw crushers where the dynamics of crushed particles are crucial in overall machine performance. On the other hand, PBM is suitable for milling simulations. Calibration of a DEM simulation requires high precision in particle shape, material property (such as the coefficient of restitution, Young‘s Modulus, rolling friction, etc.) and operational parameters such as the toggle speed, feed rate and flow rate. It has also been observed that authors such as Legendre, Khanal and Donovan did not take into account the eccentricity of the swing-jaw during comminution. Neglecting this parameter affected the end prediction of power consumption as it deviates from the realistic nature of the jaw crusher.

A single toggle jaw crusher has multiple variables that affect the overall power consumption. According to Rose and English jaw-crusher model, power is a function of toggle speed, reduction ratio and throw. To find the optimal design parameters, Genetic Algorithms have been utilised by Legendre and Lee. Even though the GAs obtain the optimal design parameters, these codes do not take into account the machine and product mechanical properties. Therefore, they must be used together with DEM for realistic predictions.

The power consumption of a jaw crusher is also dependent on the feed material‘s fracture toughness, elastic modulus and reduction ratio. For instance, high reduction ratios are often associated with high power consumption. The reduction ratio also determined the capacity and throughput of the machine [39].

Stiffeners have also been used to increase the strength to weight ratio of the swing jaw [34] [41] [47]. It has been

demonstrated that stiffeners reduce power consumption by approximately 25%. However, the optimal number of stiffeners has not been determined, and the deflections and stresses associated to stiffeners have not been accounted for. The following gaps were identified:

1) The eccentricity of the swing jaw was neglected while simulating the DEM breakage process.
2) Product and process parameters such as particle shape and flow rate have been neglected by researchers.
3) The effect of stiffeners on stresses and deflections on the swing jaw have not been fully studied. In addition, the optimal number of stiffeners has not been determined yet.
4) Inter-particle interaction has not been included in simulations by researchers.

REFERENCES

[1] P. W. Cleary, "Industrial particle flow modelling using discrete element method," *Engineering Computations*, vol. 26, no. 6, pp. 698–743, 2009.

[2] D. Legendre and R. Zevenhoven, "Assessing the energy ef fi ciency of a jaw crusher," pp. 1–12, 2014.

[3] J. Quist, "Cone Crusher Modelling and Simulation," no. 1652, 2012.

[4] P. W. Cleary and M. D. Sinnott, "Simulation of particle flows and breakage in crushers using DEM: Part 1 - Compression crushers," *Minerals Engineering*, vol. 74, pp. 178–197, 2015. [Online]. Available: http://dx.doi.org/10.1016/j.mineng.2014.10.021

[5] P. A. Cundall and O. D. L. Strack, "A discrete numerical model for granular assemblies," *Géotechnique*, vol. 29, no. 1, pp. 47–65, 1979.

[6] N. Jiménez-Herrera, G. K. Barrios, and L. M. Tavares, "Comparison of breakage models in DEM in simulating impact on particle beds," *Advanced Powder Technology*, 2017.

[7] T. Zhao, *Coupled DEM-CFD analyses of landslide-induced debris flows*. Singapore: Springer, 2017.

[8] D. O. Potyondy and P. A. Cundall, "A bonded-particle model for rock," *International Journal of Rock Mechanics and Mining Sciences*, vol. 41, no. 8 SPEC.ISS., pp. 1329–1364, 2004.

[9] J. R. Mcdowell, "DEM of triaxial tests on crushable sand," pp. 551–562, 2014.

[10] S. Lobo-Guerrero and L. E. Vallejo, "Crushing a weak granular material: experimental numerical analyses," *Géotechnique*, vol. 55, no. 3, pp. 245–249, 2005.

[11] A. R. Russell, D. Muir Wood, and M. Kikumoto, "Crushing of particles in idealised granular assemblies," *Journal of the Mechanics and Physics of Solids*, vol. 57, no. 8, pp. 1293–1313, 2009. [Online]. Available: http://dx.doi.org/10.1016/j.jmps.2009.04.009

[12] H. M. Y. Nakata, A. F. Hyde, "A probabilistic approach to sand particle crushing in the triaxial test," no. 5, pp. 567–583, 1999.

[13] D. Vallet and J. C. Charmet, "Mechanical behaviour of brittle cement grains," *Journal of Materials Science*, vol. 30, no. 11, pp. 2962–2967, 1995.

[14] W. Zheng and D. D. Tannant, "Computers and Geotechnics Grain breakage criteria for discrete element models of sand crushing under one-dimensional compression," *Computers and Geotechnics*, no. October, pp. 0–1, 2017. [Online]. Available: http://dx.doi.org/10.1016/j.compgeo.2017.10.004

[15] B. Wang, U. Martin, and S. Rapp, "Discrete element modeling of the single-particle crushing test for ballast stones," *Computers and Geotechnics*, vol. 88, pp. 61–73, 2017. [Online]. Available: http://dx.doi.org/10.1016/j.compgeo.2017.03.007

[16] S. Antonyuk, M. Khanal, J. Tomas, S. Heinrich, and L. Mörl, "Impact breakage of spherical granules: Experimental study and DEM simulation," *Chemical Engineering and Processing: Process Intensification*, vol. 45, no. 10, pp. 838–856, 2006.

[17] A. Spettl, M. Dosta, S. Antonyuk, S. Heinrich, and V. Schmidt, "Statistical investigation of agglomerate breakage based on combined stochastic microstructure modeling and DEM simulations," *Advanced Powder Technology*, vol. 26, no. 3, pp. 1021–1030, 2015. [Online]. Available: http://dx.doi.org/10.1016/j.apt.2015.04.011

[18] D. Mas Ivars, *Bonded particle model for jointed rock mass*, 2010, no. January. [Online]. Available: http://kth.diva-portal.org/smash/record.jsf?pid=diva2:300557

[19] C. S. C. Potapov, Alexander V., "A three dimensional simulation of brittle solid fracture," *International Journal of Modern Physics*, vol. Volume 7, no. No. 5.

[20] A. Paluszny, X. Tang, M. Nejati, and R. W. Zimmerman, "A direct fragmentation method with Weibull function distribution of sizes based on finite- and discrete element simulations," *International Journal of Solids and Structures*, vol. 80, pp. 38–51, 2016. [Online]. Available: http://dx.doi.org/10.1016/j.ijsolstr.2015.10.019

[21] J. Lichter, K. Lim, A. Potapov, and D. Kaja, "New developments in cone crusher performance optimization," *Minerals Engineering*, vol. 22, no. 7-8, pp. 613–617, 2009. [Online]. Available: http://dx.doi.org/10.1016/j.mineng.2009.04.003

[22] C. L. Wu, O. Ayeni, A. S. Berrouk, and K. Nandakumar, "Parallel algorithms for CFD-DEM modeling of dense particulate flows," *Chemical Engineering Science*, vol. 118, pp. 221–244, 2014.

[23] L. Vogel and W. Peukert, "From single particle impact behaviour to modelling of impact mills," *Chemical Engineering Science*, vol. 60, no. 18, pp. 5164–5176, 2005.

[24] T. Brosh, H. Kalman, and A. Levy, "Accelerating CFD-DEM simulation of processes with wide particle size distributions," *Particuology*, vol. 12, no. 1, pp. 113–121, 2014. [Online]. Available: http://dx.doi.org/10.1016/j.partic.2013.04.008

[25] P. W. Cleary, "Large scale industrial DEM modelling," *Engineering Computations*, vol. 21, no. 2/3/4, pp. 169–204, 2004. [Online]. Available: http://dx.doi.org/10.1108/02644400410519730

[26] G. Barrios, L. Tavares, and J. Pérez-Prim, "DEM Simu-

lation of Bed Particle Compression Using The Particle Replacement Model," *Proceedings of the 14th European Symposium on Comminution and Classification*, no. September, pp. 59–63, 2015.

[27] H. Li, G. McDowell, and I. Lowndes, "Discrete element modelling of a rock cone crusher," *Powder Technology*, vol. 263, pp. 151–158, 2014. [Online]. Available: http://dx.doi.org/10.1016/j.powtec.2014.05.004

[28] M. C. Weng and H. H. Li, "Relationship between the deformation characteristics and microscopic properties of sandstone explored by the bonded-particle model," *International Journal of Rock Mechanics and Mining Sciences*, vol. 56, pp. 34–43, 2012. [Online]. Available: http://dx.doi.org/10.1016/j.ijrmms.2012.07.003

[29] M. Obermayr, K. Dressler, C. Vrettos, and P. Eberhard, "A bonded-particle model for cemented sand," *Computers and Geotechnics*, vol. 49, pp. 299–313, 2013. [Online]. Available: http://dx.doi.org/10.1016/j.compgeo.2012.09.001

[30] R. Cabiscol, J. H. Finke, and A. Kwade, "Calibration and interpretation of DEM parameters for simulations of cylindrical tablets with multi-sphere approach," *Powder Technology*, 2017. [Online]. Available: https://doi.org/10.1016/j.powtec.2017.12.041

[31] N. Metta, M. Ierapetritou, and R. Ramachandran, "A multiscale DEM-PBM approach for a continuous comilling process using a mechanistically developed breakage kernel," *Chemical Engineering Science*, 2017. [Online]. Available: https://doi.org/10.1016/j.ces.2017.12.016

[32] B. A. Suresh, " Computer Aided Design and Analysis of Swing Jaw Plate of Jaw Crusher Computer Aided Design and Analysis of Swing Jaw Plate of Jaw Crusher Department of Mechanical Engineering National Institute of Technology," 2009.

[33] J. G. DONOVAN, *Fracture Toughness Based Models for The Prediction of Power Consumption, Product Size, And Capacity of Jaw Crushers*, 2003.

[34] R. S. More and G. H. Raisoni, "A Design & Analysis of Swing Jaw Plates of Jaw Crusher," vol. 3, no. 4, pp. 400–408, 2014.

[35] A. J. Magerowski, "Controlling Crushing Costs and Particle Shape."

[36] S. Sundar.V, "Optimum design and analysis of single toggle jaw crusher," vol. 8354, no. 3, pp. 194–203, 2014.

[37] R. B. Miller, "Designing A New Crushing Technique to Combine Impact and Compression Fracturing in A Rock Crushing Chamber," pp. 1–14.

[38] Y. K. Ã and N. Kotake, "Comminution Energy and Evaluation in Fine Grinding," vol. 12, no. 07, 2007.

[39] A. Gupta and D. Yan, *Introduction to Mineral Processing Design and Operation*, 2006.

[40] K. Schroe, *Production, Handling and Characterization of Particulate Materials*, 2016, vol. 25. [Online]. Available: http://link.springer.com/10.1007/978-3-319-20949-4

[41] G. Doktoringenieur, M. Khanal, M. Gutachter, T. Prof, A. B. Prof, and S. Luding, "Simulation of Crushing Dynamics of an Aggregate-Matrix Composite by Compression and Impact Stressings," no. January, 2005.

[42] D. Coley, "An introduction to genetic algorithms for scientists and engineers," p. 244, 1999.

[43] E. LEE, *Optimization of Compressive Crushing*, 2012.

[44] D. Tromans, "Mineral comminution: Energy efficiency considerations," *Minerals Engineering*, vol. 21, no. 8, pp. 613–620, 2008.

[45] T. Korman, G. Bedekovic, T. Kujundzic, and D. Kuhinek, "Impact of physical and mechanical properties of rocks on energy consumption of Jaw Crusher," *Physicochemical Problems of Mineral Processing*, vol. 51, no. 2, 2015.

[46] G. Kirankumar, "Optimization of Jaw Crusher," pp. 238–242, 2014.

[47] M. Khanal and C. T. Jayasundara, "Role of particle stiffness and inter-particle sliding friction in milling of particles," *Particuology*, vol. 16, pp. 54–59, 2014. [Online]. Available: http://dx.doi.org/10.1016/j.partic.2014.04.003